scientific reports

Check for updates

OPEN

Ab initio study of the structure, elastic, and electronic properties of $Ti_3(Al_{1-n}Si_n)C_2$ layered ternary compounds

S. T. Ahams[1,2]✉, A. Shaari[1], R. Ahmed[1,3], N. F. Abdul Pattah[1], M. C. Idris[1,4] & B. U. Haq[5]

The MAX phase materials such as layered ternary carbides that simultaneously exhibit characteristics of metallic and ceramic materials have received substantial interest in recent years. Here, we present a systematic investigation of the electronic, structural stabilities, and elastic properties of $Ti_3(Al_{1-n}Si_n)C_2$ (n = 0,1) MAX phase materials using the ab initio method via a plane-wave pseudopotential approach within generalized-gradient-approximations. The computed electronic band structures and projected density of states show that both Ti_3SiC_2 and Ti_3AlC_2 are metallic materials with a high density of states at the Fermi level emanating mainly from Ti-3d. Using the calculated elastic constants, the mechanical stability of the compounds was confirmed following the Born stability criteria for hexagonal structures. The Cauchy pressure and the Pugh's ratio values establish the brittle nature of the Ti_3SiC_2 and Ti_3AlC_2 MAX phase materials. Due to their intriguing physical properties, these materials are expected to be suitable for applications such as thermal shock refractories and electrical contact coatings.

MAX phases are a family of over 70 synthesized ternary nitrides and carbides of general stoichiometry $M_{n+1}AX_n$ where $n = 1$, 2, or 3, M denotes early transition metals (TM), A represents A- group elements (mostly from group IIIA or IVA) and X is either nitrogen (N) or carbon (C)[1–4]. Resulting from their general formula, different groups of MAX phases are characterized as 211, 312, 413, 614, and so on[5]. Some MAX phases were discovered experimentally by Nowotny et al. about forty years ago[6]. In the early 1960s, the majority of MAX phases were discovered in a succession of experiments by Nowotny and his co-workers[7]. However, these discovered MAX phases did not receive adequate interest till the Barsoum and El-Raghy synthesized and fully characterized the bulk Ti_3SiC_2 MAX phase in 1996[8]. Thereafter, interest in the layered ternary compounds increased rapidly[9–11]. Based on the web of science (WOS)[12], to date, there are over 4,168 published papers on MAX compounds alone, with Ti_3SiC_2 having roughly half of the published works in the past six years[13,14]. MAX phase family is a large group of layered ternary carbides and nitrides that crystalizes into the hexagonal structure of spacegroup No. P_{63}/mmc. Withthe characteristics of metallic as well as ceramics materials[15], where each group member contains at least two forms of ionic, covalent, or metallic chemical bonds[16]. The MAX phases such as Ti_3SiC_2 and Ti_3AlC_2 are a 312 class of layered ternaries where the individual phases differ by the number of M-layers parting the A-layers in the 312-MAX phases[17–21]. These compounds combine some characteristics of metals like strong compressive strength, high fracturing strength, hardness, ductility, good electrical and thermal conductivity, high stiffness, damage tolerance, relatively low thermal expansion coefficient. Like ceramics they have outstanding thermal and chemical tolerance. . Furthermore, these compounds are considered as one of the best classes of materials for coating on steel surfaces in heavy liquid metals and as pump impellers. However, Ti_3SiC_2 and Ti_3AlC_2 are among the best-accepted representatives of the MAX phase compounds and are known as the best thermal conductors than titanium metal[22–26].

First-principles approaches are widely employed to study the properties of MAX phases, for example, M_2GaN (M = Ti, V and Cr)[27], Ti_2TlC, Zr_2TlC, and Hf_2TlC[17,23], Ti_3AlC_2 and Ti_2SiC_2[20]. Zhou et al.[28] reported the

[1]Department of Physics, Faculty of Science, Universiti Teknologi Malaysia, UTM Skudai, 81310 Johor Bahru, Johor, Malaysia. [2]Department of Pure and Applied Physics, Faculty of Science, Adamawa State University, Mubi, Nigeria. [3]Center for High Energy Physics, University of the Punjab, Quaid-E-Azam Campus, Lahore 54590, Pakistan. [4]Department of Physics, Sule Lamido University, Kafin Hausa, Jigawa State, Nigeria. [5]Advanced Functional Materials and Optoelectronics Laboratory (AFMOL), Department of Physics, Faculty of Science, King Khalid University, P.O. Box 9004, Abha, Saudi Arabia. ✉email: stahams@gmail.com

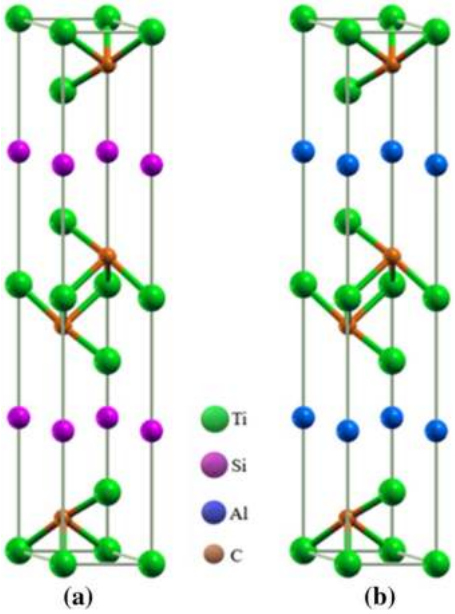

Figure 1. Crystal structure of (**a**) Ti_3AlC_2, (**b**) Ti_3SiC_2 MAX phase compounds.

distribution of charge density on the (1120) plane of Ti_3AlC_2, where robust directional Ti-C-Ti-C-Ti covalent bond chains were observed that linked to fairly weaker Ti–Al covalent bindings. In a similar study of electronic structure and bonding properties of Ti_3AlC_2, Wang and Zhou[29] reported that the electrical conductivity of Ti_3AlC_2 decreases with increasing pressure, and over the whole pressure range, the material was found to exhibit elastic anisotropy. Son et al.[30] have used density functional theory (DFT) to analyze the structural, elastic, and thermodynamic properties of Ti_3SiC_2 and Ti_3AlC_2 crystals. In order to discover the finite-temperature properties of these crystals, the vibrational, mechanical, quasi-harmonic contributions, and anharmonic adjustment to the total free energy of the systems were determined and extrapolated and the functions of electron localization, charge densities, electronic and vibrational densities have been studied.

Zhou and Zhimei investigated the electronic structure and chemical bonding in layered machinable Ti_3SiC_2[31]. According to them, bonding within Ti_3SiC_2 is facilitated by metallic, covalent, and ionic bonding due to the strong Ti-C-Ti-C-Ti covalent bond strings in the structure[31]. In recent years, several studies have been carried out on the mechanical properties, and structural stabilities of Ti_3SiC_2 and Ti_3AlC_2[32–34] that reported their excellent structural properties that are suitable for many practical applications. Synchrotron x-ray diffraction measurements showed that Ti_3SiC_2 and Ti_3AlC_2 are stable materials under pressure from 0 to 61 GPa at room temperature[35]. Thermal stability of bulk Ti_3AlC_2 has been investigated[36] within 1100–1400 °C, and hydrogen has been found to alter the properties and stability of the MAX phase. Analogous facts have also been noticed in the temperature range 1473–1673 K in bulk Ti_3SiC_2 in the hydrogen atmosphere and it was found that the dissociation of Ti_3SiC_2 was accelerated by hydrogen[37].

Herein, we have investigated Ti_3SiC_2 and Ti_3AlC_2 using plane-wave pseudopotentials (PW-PP) approach in the framework of DFT. Since hardness varies from one material to another as commonly acknowledged by materials scientists, materials with Vickers hardness greater than 40 GPa are categorized as superhard[38,39]. We have achieved a result which by far characterizes Ti_3SiC_2 and Ti_3AlC_2 as superhard materials which we feel none of the studies conducted so far could address.

Result and discussion

Structural properties. The layered ternary $Ti_3(Al_{1-n}Si_n)C_2$ (n = 0, 1) compounds are based on the layers of hexagonally close-packed Si/Al and Ti layers with C occupying octahedral centers between the Ti layers as depicted in Fig. 1. The end phases could also be characterized as alternating stacking of two layers of a planar close-packed Si/Al and Ti_6C octahedral layers. The Ti atom is found to be located at 4f. (0.33, 0.67, *z*), Al/Si atoms are positioned at 2b (0, 0, 0.25) whereas the atom of C is at 4f. (0.33, 0.67, *z*) Wyckoff positions. Figure 1 illustrates the crystal symmetries of the studied compounds and their computed structural parameters as well as the experimental results from available literature(s) are summarized in Table 1. The results of the equilibrium lattice constants, bulk modulus, and its pressure derivative are computed by fitting the obtained data of the equilibrium energy as well as volume to the second-order Birch-Murnaghan's equation of state (EOS)[40]. The obtained results showed the reasonability of our calculations.

$$E(V) = E_o \frac{9}{16} B_o \left[\left(4 - B_o^{'}\right) \frac{V_o^3}{V^2} - \left(14 - 3B_o^{'}\right) \frac{V_o^{7/3}}{V^{4/3}} \left(16 - 3B_o^{'}\right) \frac{V_o^{5/3}}{V^{2/3}} \right] \quad (1)$$

Compound	Reference	a (Å)	c (Å)	c/a	V (Å^3)	B_o (GPa)	$B_o^{'}$
Ti_3AlC_2	This work	3.0781	18.7681	6.0973	153.93	145	2.81
	Exp.[41]	3.082	18.642	6.0487			
	Calc.[30]	3.083	18.652	6.040		163.35	
Ti_3SiC_2	This work	3.0697	17.6864	5.7000	145.60	180.5	4.14
	Exp.[41]	3.075	17.734	5.7672			
	Calc.[30]	3.077	17.715	5.7572		192.61	

Table 1. Calculated equilibrium lattice parameters *a, c, c/a* ratio, volume, *V*, bulk modulus B_o, and its pressure derivative, $B_o^{'}$ and values from the literature.

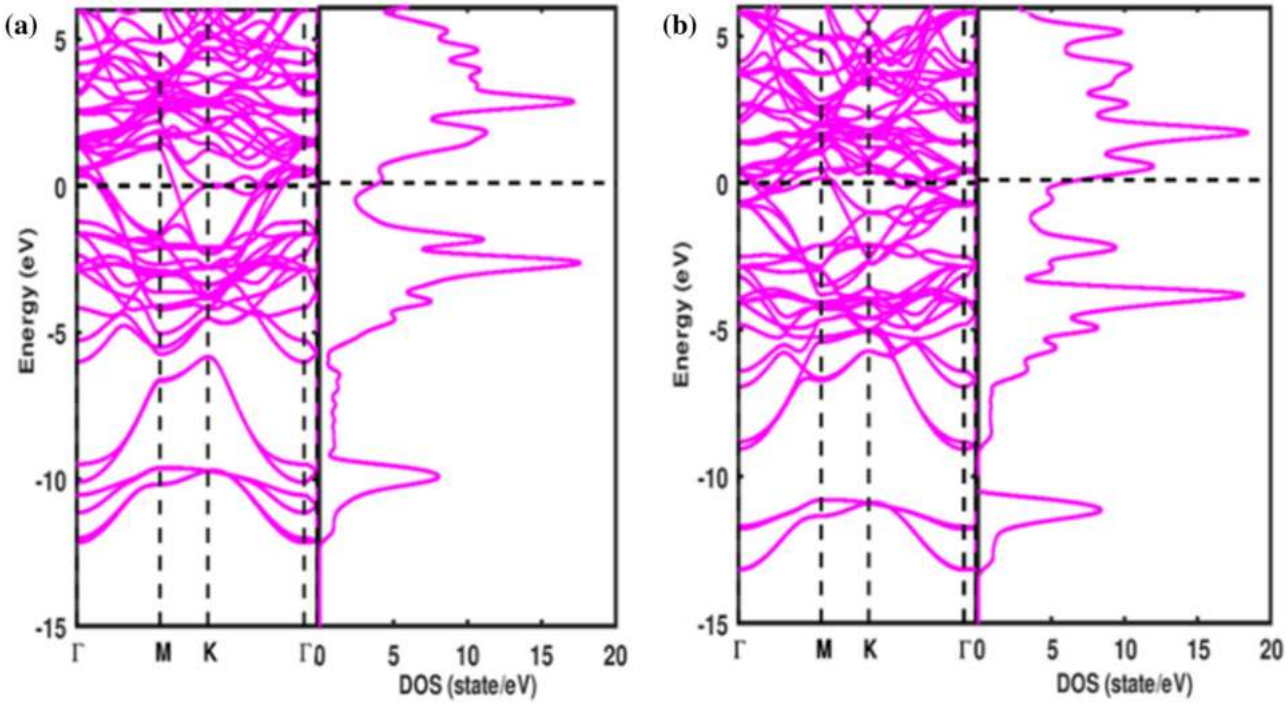

Figure 2. Band structures and TDOS of (**a**) Ti_3SiC_2, (**b**) Ti_3AlC_2 MAX phase compounds.

One can easily note that the difference between our obtained results and experimental data of equilibrium lattice parameters is less than 1%, showing that our results obtained at the level of the Perdew-Burke-Ernzerhof (PBE) type of generalized gradient approximations functional are sufficiently reliable. In Table 1, the bulk modulus of Ti_3SiC_2 is higher than that of Ti_3AlC_2, showing that Ti_3SiC_2 is harder than Ti_3AlC_2.

Electronic properties. Figure 2 demonstrates the band structures and total density of states (TDOS) computed along the high symmetry points in the brilluoin zone (BZ) using the equilibrium lattice parameters. It is seen that both valence bands and conduction bands overlap significantly resulting in no energy gap at the Fermi level. Thus, the studied compounds demonstrate metallic character which is a common feature of the MAX phase materials. However, there are more valence electrons in the Ti_3SiC_2 unit cell than in Ti_3AlC_2. This gives rise to the further occupation of the bonding states near the Fermi level. The substitution of Si by Al in Ti_3AlC_2 presents additional valence electrons per atom, and consequently, the Fermi level is moved to a higher energy level. This suggests that the increased extra valence electrons fill in the Si/Al-Ti *p-d* hybridized bonding states as well as the metal to metal *d-d* consequential bonding.

Accordingly, the filling of the bonding orbitals rises the strength of the bond and thereby increasing the bulk moduli. The energy band also exhibits a highly anisotropic character along with lesser *c*-axis energy dispersion. The anisotropy of the band structure near and below the Fermi level implies that, for single crystals, both Ti_3SiC_2 and Ti_3AlC_2 are conductors and anisotropic, and electrical conductivity is lowered along *c* direction than the *ab*- plane similar to the observed trend in the literature[28].

The investigated total densities of states (TDOS) plot for Ti_3SiC_2 and Ti_3AlC_2 presented in Fig. 2 points out that the peak structures and corresponding heights of the peaks are equivalent, signifying resemblance in chemical bonding. The TDOS per unit cell at the Fermi level for Ti_3SiC_2 and Ti_3AlC_2 are 4.029 and 6.855 states/eV, respectively. Therefore, there is an increasing trend in the DOS at the Fermi level with an increasing number of

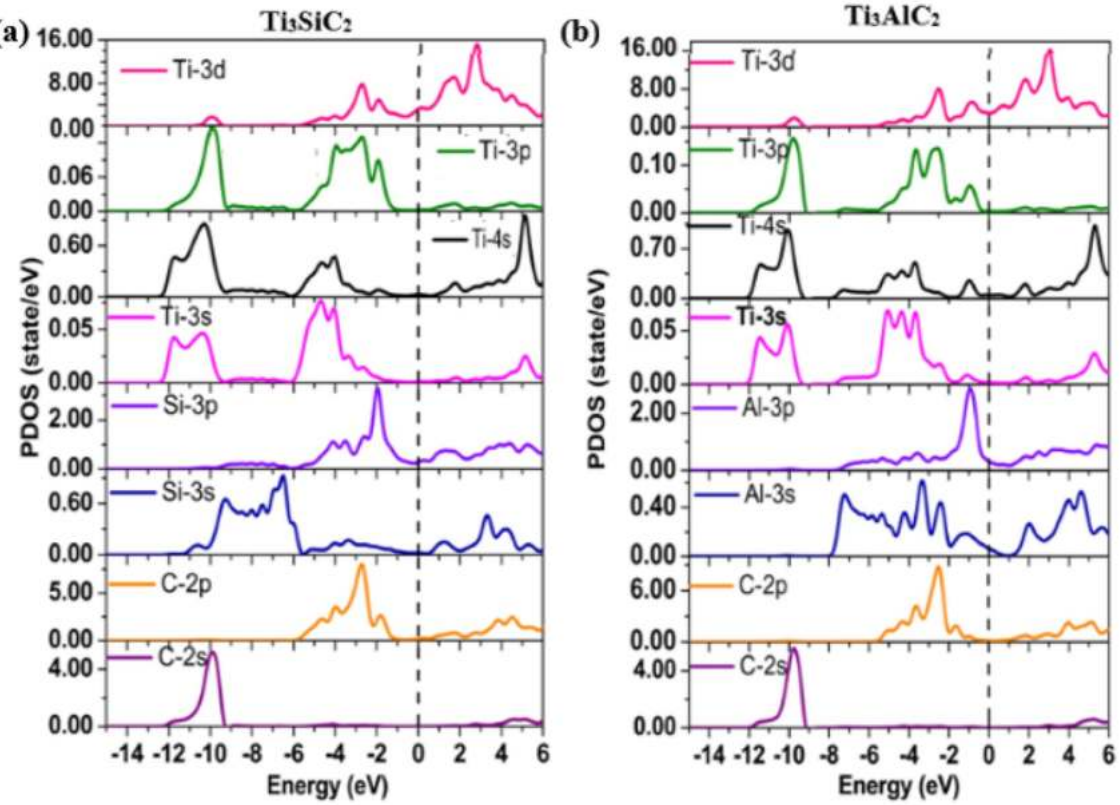

Figure 3. Calculated PDOS of (**a**) Ti_3SiC_2 and (**b**) Ti_3AlC_2 MAX phases.

Comp	*XC*	C_{11}	C_{12}	C_{13}	C_{33}	C_{44}	Refs.
Ti_3AlC_2	PBE	277	93	70	242	114	This work
	Exp	361	75	70	299	124	[47]
	Others	353	75	69	296	119	[47]
Ti_3SiC_2	PBE	326	98.3	115	317	143	This work
	Exp	365	125	120	375	122	[47]
	Others	366	94	100	352	153	[47]

Table 2. Computed elastic constants C_{ij} (GPa) alongside experimental and theoretical results.

valence electrons of the transition metals showing that the transition metal bands play a dominant role in the TDOS and their electrical transport properties. Analysis of bonding properties is obtained from the PDOS of each contributing element in Fig. 3. Here, the width of Al-3 s and Si-3 s states are wider for each one than that of the C-2 s state. With several less contributing peaks in the Al/Si-are due to 3 s states. The Al/Si-3 s energy states show that there are *s-p* interactions in Al/Si, i.e. close-packed layer of Al/Si atoms are bonded through *s-p* interactions. For the energy range -12 eV to -9.4 eV in the valence bands of both Ti_3SiC_2 and Ti_3AlC_2, there is a high degree of hybridization of C-2p with Ti-3d states, which suggests covalent bonding between them. Hence the chemical stability is largely attributed to the *p-d* hybridization. Therefore, the Ti-3d and C-2p hybridization is a driving bonding force in Ti_3SiC_2 and Ti_3AlC_2, similar to bonding properties in some 312 MAX phases like Ti_3SnC_2 and Ti_3GeC_2[42,43].

Elastic properties. Investigations of elastic constants are vital for applications related to the mechanical properties of solids. They provide information on stability, bonding, ductility, brittleness, anisotropy, compressibility, Vicker's hardness, and stiffness of solids[44,45]. For hexagonal crystals structures, five independent elastic constants ($C_{11}, C_{12}, C_{13}, C_{33}, C_{44}$) are required. Table 2 summarizes our computed results of the five independent elastic constants of Ti_3SiC_2 and Ti_3AlC_2 alongside available experimental and theoretical data.

A stable hexagonal crystal must satisfy the following Born-Huang stability criteria[46];

$$C_{11} > 0; C_{11} - C_{12} > 0; C_{44} > 0; (C_{11} + C_{12})C_{33} - 2C_{13}^2 > 0 \quad (2)$$

Comp	B	Y	G	η	B^{-1}	B/G	C_c	A	H_V	Refs.
Ti_3AlC_2	139	215	87	0.24	0.007	1.60	− 44	1.203	40.28	This work
	161.2	321	132	0.178	0.006	1.22	− 50	0.971	36.88	[18,47]
Ti_3SiC_2	189	297	121	0.23	0.005	1.56	− 28	1.398	46.75	This work
	203.9	307	123	0.248	0.005	1.66	− 53	1.202	25.53	[18,47]

Table 3. Computed bulk modulus B (GPa), Young modulus Y(GPa), shear modulus G (GPa), Poisson's ratio η, compressibility B^{-1} (GPa)$^{-1}$, Pugh's ratio (B/G), Cauchy pressure C_c(GPa), anisotropic factor-A and Vicker's hardness H_v.

Table 2 demonstrates that the computed results of the independent elastic constants for Ti_3SiC_2 and Ti_3AlC_2 MAX phase compounds satisfy the mechanical stability criteria which signify that all the compounds are mechanically stable. It is also well known that elastic constants C_{11}, and C_{33} shows linear compression resistances along a and c directions, respectively, whereas C_{12}, $C_{13,}$ and C_{44} are related to the shape elasticity. Consistent with Table 2, the value of C_{11} is higher than C_{33} for both Ti_3SiC_2 and Ti_3AlC_2 compounds which agrees well with literature results.

From the computed elastic constants, several polycrystalline elastic moduli comprising, Bulk, Shear, Young moduli, and Poisson's ratio were evaluated using Voigt[48], Reuss[49], and Hill[50] approximations. It is assumed that, in the Voigt scheme, the strain is uniform all along the polycrystalline materials aggregating to external strain. By following this approach, for the hexagonal lattices, the Voigt shear modulus (G_V) and Reuss shear modulus (G_R) are expressed as:

$$G_V = \frac{1}{15}\{2C_{11} - C_{12} + C_{33} - 2C_{13}\} + \frac{1}{5}\left\{2C_{44} + \frac{1}{2}(C_{11} - C_{12})\right\} \tag{3}$$

$$G_R = \frac{5}{2}\left\{\frac{\left[\left[(C_{11} + C_{12})C_{33} - 2C_{13}^2\right]C_{44}C_{66}\right]}{\left[3B_V C_{44}C_{66} + \left[(C_{11} + C_{12})C_{33} - 2C_{13}^2\right](C_{44} + C_{66})\right]}\right\} \tag{4}$$

And Voigt bulk modulus (B_V), Reuss bulk modulus (B_R) by:

$$B_V = \frac{1}{9}\{2(C_{11} + C_{12}) + C_{33} + 4C_{13}\} \tag{5}$$

$$B_R = \frac{(C_{11} + C_{12})C_{13} - 2C_{13}^2}{C_{11} + C_{12} + 2C_{33} + 4C_{13}} \tag{6}$$

Hill showed that Voigt/Reuss averages give upper and lower bounds, and therefore, proposed that real effective moduli can be approximated by the arithmetic mean of the two bounds[51]. Thus, using Hill's approximations

$$B = \frac{1}{2}(B_R + B_V), \quad G = \frac{1}{2}(G_R + G_V) \tag{7}$$

We have also computed Y, and η, which are commonly evaluated for polycrystalline materials to study their hardness. Both Y and η are defined by the following expressions as;

$$Y = \frac{9BG}{3B + G}, \quad \eta = \frac{3B - 2G}{2(3B + G)} \tag{8}$$

The computed Bulk modulus, Young's modulus, Shear moduli, and Poisson's ratio of both Ti_3SiC_2 and Ti_3AlC_2 as defined in Eqs. (3)–(8) are listed in Table 3. The calculated values for the bulk modulus of Ti_3SiC_2 and Ti_3AlC_2 are 139 GPa and 182 GPa respectively. These values agree well with the reported value by Gray et al.[47], with less than 13% and 7% deviation respectively for Ti_3AlC_2 and Ti_3SiC_2. Moreover, our results for Shear modulus of 87 GPa for Ti_3AlC_2 although are lower than the reported experimental value in Table 3, the results of Ti_3SiC_2 of 121 GPa are in good agreement with the reported value. From comparing Tables 1 and 3, it can be seen that the calculated value of B obtained from the single crystal elastic constants summarized in Table 3 has approximately the same value as the one obtained from the data fitting in the Murnaghan's equation of state (Table 1). This indicates the accuracy and reliability of our computed elastic constants for both Ti_3SiC_2 and Ti_3AlC_2 MAX phase compounds.

Following the Pugh ratio, B/G shows the brittle or ductile character of materials. Pugh's critical value is 1.75. The calculated ratio B/G for Ti_3AlC_2 and Ti_3SiC_2 are 1.60 and 1.56, respectively, which are less than Pugh's critical value. As such, these compounds have a brittle feature which agreed well with the result given in Table 3[52]. Cauchy relation defined as: $C_c = C_{13} - C_{44}$, is another parameter signifying ductility or brittleness of a material. Positive values of C_c shows ductility otherwise the material is brittle[53]. The evaluated C_c of the ternaries are -44 and -28 GPa respectively. From these values, one can conclude that the studied materials are brittle in nature

which confirmed the Pugh's result. Consequently, the brittle nature of Ti_3AlC_2 and Ti_3SiC_2 can be related to their ceramic character.

Young's modulus (Y) measures the stiffness of a material. The higher the Y, the stiffer a material is. Our result presented in Table 3 shows that there is good agreement with the reported values of 215 GPa and 297 GPa for Ti_3AlC_2 and Ti_3SiC_2, respectively. Information about the bonding forces can be obtained via Poisson's ratio (η). The(η) for Ti_3AlC_2 and Ti_3SiC_2 are 0.24 and 0.23 respectively, which shows the interatomic forces within studied materials are central since upper and lower limits of the Poisson's ratio is 0.5 and 0.25 respectively, and the calculated values fall within the two limits. Our results are closer to the experimental value of 0.178 for Ti_3AlC_2 and 0.248 for Ti_3SiC_2[52]. We have further calculated the Vickers' hardness H_v[54] of studied compounds. Vickers's hardness is another key mechanical property of solids that explains stability, which is predicted using Eq. (9). It is reported that solids with Vickers hardness $H_V > 40$ GPa[38] are graded as super hard solids. The calculated H_v of Ti_3AlC_2 and Ti_3SiC_2 MAX phase compounds are 40.28 GPa, and 46.75 GPa respectively (Table 3). Therefore, these crystals, have an excellent ability to withstand dents or scratches.

$$H_V = 0.92\left(\frac{B}{G}\right)^{1.3137} G^{0.708} \tag{9}$$

Method

Ab initio calculations were used to investigate the elastic, and electronic properties of Ti_3SiC_2 and Ti_3AlC_2 using PW-PP as implemented in Quantum Espresso[55]. Generalized gradient approximation (GGA) parametrized by Perdew-Burke-Ernzerhof (PBE) is used to treat exchange and correlation (XC) energy[56]. The core ion and valence electrons interactions were described using ultrasoft-pseudopotentials (UPP). A 600 Ry kinetic energy cut-off of the plane wave is used in the calculations. The electronic configurations: $3s^2$, $4s^2$, $3p^6$, $3d^2$ for Ti, $3s^2$, $3p^2$ for Si, $3p^1$, $3s^2$ for Al and $2s^2$, $2p^2$ for C were considered for the valence electrons. For the Brillouin zone (BZ) integration, $12 \times 12 \times 12$ k-points mesh was generated using the Monkhorst–Pack scheme[57]. These parameters were found to be adequate to converge total energies up to 10^{-8} eV. Both studied materials were fully relaxed in terms of cell parameters and atomic positions. Analysis of independent elastic constant (C_{ij}) were performed using thermo_pw[45]. C_{ij} delineates response of materials to macroscopic stress. In computing elastic constants, a small strain, e is applied to a material and the variation of total energy per volume, U of the material is obtained[58]:

$$U = \frac{\Delta E}{V_0} = \frac{1}{2}\sum_{i}^{n}\sum_{j}^{m} C_{ij} e_i e_j \tag{10}$$

where V_0 and ΔE represent the equilibrium volume and the difference between the initial and deformed total energy of the system respectively. The hexagonal Ti_3SiC_2 and Ti_3AlC_2 MAX phase compounds are characterized by five independent elastic constants which include C_{11}, C_{12}, C_{13},C_{33} and C_{44}. Therefore, the elastic matrix of the hexagonal system is written as[59,60];

$$C_{ij} = \begin{bmatrix} C_{11} & C_{12} & C_{13} & . & . & . \\ . & C_{11} & C_{13} & . & . & . \\ . & . & C_{33} & . & . & . \\ . & . & . & C_{44} & . & . \\ . & . & . & . & C_{44} & . \\ . & . & . & . & . & . \end{bmatrix} \tag{11}$$

Conclusion

In this work, the structural stability, electronic, and mechanical properties were investigated using ab-initio calculations. The complete set of independent elastic constants C_{ij}, shear modulus, bulk modulus, Poisson's ratio, and Young's modulus were calculated. Our results showed that the studied ternaries are mechanically stable and are super hard materials with Vicker's hardness as large as 46.75 GPa and 40.28 GPa for Ti_3SiC_2 and Ti_3AlC_2 respectively. The investigated electronic band structures, TDOS, and PDOS showed the metallic behavior of these compounds. In Ti_3SiC_2, the top of the VB and bottom of the CB were found to be dominated by the Si-3p, C-2p, and Ti-3d energy states while for the Ti_3AlC_2 the top and bottom of VB and CB were respectively found to be shaped by Al-3p, C-2p, and Ti-3d orbitals. We expect that our findings will provide suitable guidance for experimental and theoretical studies on these interesting MAX phases.

Received: 3 December 2020; Accepted: 16 February 2021

References

1. Kulkarni, S. R. *et al.* High-temperature thermal expansion and stability of V2AlC Up to 950 °C. *J. Am. Ceram. Soc.* **90**, 3013–3016 (2007).
2. Lapauw, T. *et al.* Synthesis of MAX phases in the Hf-Al-C system. *Inorg. Chem.* **55**, 10922–10927 (2016).
3. Lapauw, T. *et al.* The double solid solution (Zr, Nb) 2(Al, Sn)CMAX phase: a steric stability approach. *Sci. Rep.* **2**, 1–13 (2018).
4. Roknuzzaman, M. *et al.* Physical properties of predicted Ti 2 CdN versus existing Ti 2 CdC MAX phase: an ab initio study. *Comput. Mater. Sci.* **113**, 148–153 (2016).
5. Eklund, P., Beckers, M., Jansson, U., Högberg, H. & Hultman, L. The Mn + 1AXnphases: materials science and thin-film processing. *Thin Solid Films* **518**, 1851–1878 (2010).

6. Nowotny, H. Struktuchemie einiger verbindungen der ubergangsmetalle mit den elementen C, Si, Ge, Sn. *Prog. Solid State Chem.* **2**, 27–62 (1970).
7. Nowotny, H. & Benesovsky, F. 13.3 Carbides W (1963).
8. Barsoum, M. W. & El-Raghy, T. Synthesis and characterization of a remarkable ceramic: Ti_3SiC_2. *J. Am. Ceram. Soc.* **79**, 1953–1956 (1996).
9. Chen, D., Tian, X., Wang, H. & Huang, Z. Rapid synthesis of bulk Ti_3AlC_2 by laser melting. *Mater. Lett.* **129**, 98–100 (2014).
10. Chin, Y. & Tuan, W. Contribution of plastic deformation of Ti_3SiC_2 to the crack deflection in the Al_2O_3/Ti_3SiC_2 composites. *Mater. Sci. Eng. A* **528**, 3270–3274 (2011).
11. Cuskelly, D. T., Richards, E. R., Kisi, E. H. & Keast, V. J. Journal of solid state chemistry Ti_3GaC_2 and Ti_3InC_2: First bulk synthesis, DFT stability calculations and structural systematics. *J. Solid State Chem.* **230**, 418–425 (2015).
12. Web of Sciences. MAX Phase.
13. Fashandi, H. *et al.* Single-step synthesis process of Ti_3SiC_2 ohmic contacts on 4H-SiC by sputter-deposition of Ti. 53–56 (2015).
14. Zhu, M., Wang, R., Chen, C., Zhang, H. & Zhang, G. Electrochemical study on the corrosion behavior of Ti_3SiC_2 in 35% NaCl solution. *RSC Adv.* **7**, 12534–12540 (2017).
15. Bai, Y., Srikanth, N., Chua, C. K. & Zhou, K. Density functional theory study of Mn + 1AXn phases : a review density functional theory study of M n + 1 AX n phases : A review. *Crit. Rev. Solid State Mater. Sci.* 1–52 (2019).
16. Li, X., Cui, H. & Zhang, R. Structural, optical, and thermal properties of MAX-phase Cr_2AlB_2. **13**, 1–9 (2018).
17. Bouhemadou, A. Structural, electronic and elastic properties of Ti2TlC, Zr2TlC and Hf2TlC. *Open Phys.* **7**, 753–761 (2009).
18. Atikur Rahman, M. Study on structural, electronic, optical and mechanical properties of MAX phase compounds and applications review article. *Am. J. Mod. Phys.* **4**, 75 (2015).
19. Velasco, B., Gordo, E., Hu, L., Radovic, M. & Tsipas, S. A. Influence of porosity on elastic properties of Ti_2AlC and Ti_3SiC_2 MAX phase foams. *J. Alloys Compd.* **764**, 24–35 (2018).
20. Li, X., Xie, X., Gonzalez-Julian, J., Malzbender, J. & Yang, R. Mechanical and oxidation behavior of textured Ti_2AlC and Ti_3AlC_2 MAX phase materials. *J. Eur. Ceram. Soc.* **40**, 5258–5271 (2020).
21. Heinzel, A., Weisenburger, A. & Müller, G. Long-term corrosion tests of Ti_3SiC_2 and Ti_2AlC in oxygen containing LBE at temperatures up to 700 °C. *J. Nucl. Mater.* **482**, 114–123 (2016).
22. Ali, M. A. S., Ali, M. A. S. & Uddin, M. M. Structural, elastic, electronic and optical properties of metastable MAX phase Ti_5SiC_4 compound. *Indian J. Pure Appl. Phys.* **54**, 386–390 (2016).
23. Bai, Y., Srikanth, N., Chua, C. K. & Zhou, K. Density functional theory study of M n+1 AX n phases: A review. *Crit. Rev. Solid State Mater. Sci.* **44**, 56–107 (2019).
24. Radovic, M. & Barsoum, M. W. MAX phases: Bridging the gap between metals and ceramics. *Am. Ceram. Soc. Bull.* **92**, 20–27 (2013).
25. Chlubny, L., Lis, J., Chabior, K., Chachlowska, P. & Kapusta, C. Processing and properties of max phases-based materials using SHS technique. *Arch. Metall. Mater.* **60**, 859–863 (2015).
26. Lapauw, T. *et al.* The double solid solution (Zr, Nb)2(Al, Sn)C MAX phase: A steric stability approach. *Sci. Rep.* **8**, 1–13 (2018).
27. Bouhemadou, A. Structural, electronic and elastic properties of MAX phases M2GaN (M = Ti, V and Cr). *Solid State Sci.* **11**, 1875–1881 (2009).
28. Zhou, Y. C., Wang, X. H., Sun, Z. M. & Chen, S. Q. Electronic and structural properties of the layered ternary carbide Ti_3AlC_2. *J. Mater. Chem.* **11**, 2336–2340 (2001).
29. Wang, J. Y. & Zhou, Y. C. Ab initio investigation of the electronic structure and bonding properties of the layered ternary compound Ti_3SiC_2 at high pressure. *J. Phys. Condens. Matter* **15**, 1983–1991 (2003).
30. Son, W. *et al.* Ab-initio investigation of the finite-temperatures structural, elastic and thermodynamic properties of Ti_3AlC_2 and Ti_3SiC_2. *Comput. Mater. Sci.* **124**, 420–427 (2016).
31. Zhou, Y. & Sun, Z. Electronic structure and bonding properties in layered ternary carbide Ti_3SiC_2. *J. Phys. Condens. Matter* **12**, L457–L462 (2000).
32. Surucu, G. Investigation of structural, electronic, anisotropic elastic, and lattice dynamical properties of MAX phases borides: An Ab-initio study on hypothetical M2AB (M = Ti, Zr, Hf; A = Al, Ga, In) compounds. *Mater. Chem. Phys.* **203**, 106–117 (2018).
33. Jiang, X., Zhao, J., Aimin, W. & Bai, Y. Mechanical and electronic properties of B-12-based ternary crystals of orthorhombic phase My IOPscience Mechanical and electronic properties of B12-based ternary crystals of orthorhombic phase this article has been downloaded from IOPscience. *Please SCRO.* https://doi.org/10.1088/0953-8984/22/31/315503 (2010).
34. Son, W. *et al.* Ab-initio investigation of the finite-temperatures structural, elastic, and thermodynamic properties of Ti_3AlC_2 and Ti_3SiC_2. *Comput. Mater. Sci.* **124**, 420–427 (2016).
35. Onodera, A., Hirano, H., Yuasa, T., Gao, N. F. & Miyamoto, Y. Static compression of Ti_3SiC_2 to 61 GPa. *Appl. Phys. Lett.* **74**, 3782–3784 (1999).
36. Chen, C., Zhang, H., Peng, S., Long, X. & Zhu, J. High-temperature hydrogenation behavior of titanium aluminum carbide. *Cailiao Yanjiu Xuebao/Chin. J. Mater. Res.* **28**, 858–864 (2014).
37. Chen, C. *et al.* High-temperature hydrogenation behaviour of bulk titanium silicon carbide. *Adv. Appl. Ceram.* **115**, 288–293 (2016).
38. Tian, Y., Xu, B. & Zhao, Z. Microscopic theory of hardness and design of novel superhard crystals. *Int. J. Refract. Met. Hard Mater.* **33**, 93–106 (2012).
39. Xu, B. & Tian, Y. Superhard materials: recent research progress and prospects. *Sci. China Mater.* **58**, 132–142 (2015).
40. Murnaghan, F. D. The compressibility of media under extreme pressure. *Physics (College. Park. Md.)* **30**, 244–247 (1944).
41. Wang, H. *et al.* First-principles study of vacancies in Ti_3SiC_2 and Ti_3AlC_2. *Materials (Basel).* **10** (2017).
42. Rayhan, M. A., Ali, M. A., Naqib, S. H. & Islam, A. K. M. A. First-principles study of vickers hardness and thermodynamic properties of Ti_3SnC_2 polymorphs. *J. Sci. Res.* **7**, 53–64 (2015).
43. Hadi, M. A. *et al.* First-principles prediction of mechanical and bonding characteristics of new T2 superconductor Ta5GeB2. *Phys. Status Solidi Basic Res.* **253**, 2020–2026 (2016).
44. Malica, C. & Dal Corso, A. Temperature-dependent atomic B factor: An ab initio calculation. *Acta Crystallogr. Sect. A Found. Adv.* **75**, 624–632 (2019).
45. Dal Corso, A. Elastic constants of beryllium: A first-principles investigation. *J. Phys. Condens. Matter* **28** (2016).
46. Mouhat, F. & Coudert, F. X. Necessary and sufficient elastic stability conditions in various crystal systems. *Phys. Rev. B Condens. Matter Mater. Phys.* **90**, 3 (2014).
47. Gray, V., Kisi, E. H., Kirstein, O. & Stampfl, A. P. J. Elastic constants of polycrystalline Ti_3AiC_2 and Ti_3SiC_2 measured using coherent inelastic neutron scattering. *J. Am. Ceram. Soc.* **100**, 705–712 (2017).
48. Voigt, W. *Lehrbuch der Kristallphysik* (Vieweg+Teubner Verlag, Wiesbaden, 1966). https://doi.org/10.1007/978-3-663-15884-4.
49. Chung, D. H. & Buessem, W. R. The Voigt-Reuss-Hill approximation and elastic moduli of polycrystalline MgO, CaF 2, β-ZnS, ZnSe, and CdTe. *J. Appl. Phys.* **38**, 2535–2540 (1967).
50. Hill, R. The elastic behaviour of a crystalline aggregate. *Proc. Phys. Soc. Sect. A* **65**, 349–354 (1952).
51. Bouhemadou, A. First-principles study of structural, electronic and elastic properties of Nb_4AlC_3. *Brazilian J. Phys.* **40**, 52–57 (2010).
52. Isaak, D. G., Graham, E. K., Bass, J. D. & Wang, H. The elastic properties of single-crystal fayalite as determined by dynamical measurement techniques. *Pure Appl. Geophys. PAGEOPH* **141**, 393–414 (1993).

53. Rubel, M. H. K. *et al.* First–principles study: Structural, mechanical, electronic and thermodynamic properties of simple–cubic–perovskite $(Ba_{0.62}K_{0.38})(Bi_{0.92}Mg_{0.08})O_3$. *Solid State Commun.* **288**, 22–27 (2019).
54. Liu, Z. T. Y., Gall, D. & Khare, S. V. Electronic and bonding analysis of hardness in pyrite-type transition-metal pernitrides. *Phys. Rev. B Condens. Matter Mater. Phys.* **90**, 1–11 (2014).
55. Giannozzi, P. *et al.* QUANTUM ESPRESSO: A modular and open-source software project for quantum simulations of materials. *J. Phys. Condens. Matter* **21** (2009).
56. Perdew, J. P., Burke, K. & Ernzerhof, M. Generalized gradient approximation made simple. *Phys. Rev. Lett.* **77**, 3865–3868 (1996).
57. Pack, H. J. M. Special points for Brillonin-zone integrations. *Phys. Rev. B* **13**, 1748–1749 (1976).
58. Asadi, Y. & Nourbakhsh, Z. First principle study of the structural, electronic, vibrational, thermodynamic, linear and nonlinear optical properties of zinc-blende ZnSe and ZnTe semiconductors. *Comput. Condens. Matter* **19**, e00372 (2019).
59. Liu, Z., Li, H., Fan, C. & Luo, W. Necessary and sufficient elastic stability conditions in 21 quasicrystal Laue classes. *Eur. J. Mech. A/Solids* **65**, 30–39 (2017).
60. Mouhat, F. & Coudert, F.-X. Necessary and sufficient elastic stability conditions in various crystal systems. *Phys. Rev. B* **90**, 224104 (2014).

Acknowledgements

The authors wish to acknowledge the support from the Ministry of Higher Education Malaysia through the Universiti Teknologi Malaysia under Grant No. R.J13000.7854.5F231. The author (Bakhtiar Ul Haq) extends his appreciation to the Deanship of Scientific Research at King Khalid University for support through Research Groups Program under Grant No. R.G.P. 2./126/42. We appreciate the Scientific Computing, and Instrumentation (SCnl) group, Department of Physics, Universiti Teknologi Malaysia, for using their research facilities. S. T. Ahams extends acknowledgment to TETFund, and Adamawa State University, Mubi, Nigeria for Scholarship support and award of the fellowship. The authors are grateful to Dr. Yap Yung Szen a Senior Lecturer and researcher of the Physics Department, for his professional and technical advice. We are grateful for Dr. Radzwan Afiq for technical assistance.

Author contributions

S.T.A. Performed the calculations, and preparation of the original draft. A.S., R.A. and B.U.H. validated the input files, supervised the calculations,and approved the final manuscript. M.C.I. and N.F.A. drew figures and tables. All authors were involved in the interpretations, reviewing and proofreading of manuscript.

Competing interests

The authors declare no competing interests.

Additional information

Correspondence and requests for materials should be addressed to S.T.A.

Reprints and permissions information is available at www.nature.com/reprints.

Publisher's note Springer Nature remains neutral with regard to jurisdictional claims in published maps and institutional affiliations.